X-ray, ^{31}P CP/MAS, and Single-Crystal NMR Studies, and ^{31}P DFT GIAO Calculations of Inclusion Complexes of Bis[6-*O*,6-*O*′-(1,2:3,4-Diisopropylidene-α-D-galactopyranosyl)thiophosphoryl] Disulfide: The Importance of C–H···S=P Contacts in the Solid State

Marek J. Potrzebowski,*[a] Gisbert Grossmann,[b] Katarzyna Ganicz,[a] Sebastian Olejniczak,[a] Włodzimierz Ciesielski,[a] Anna E. Kozioł,[c] Irena Wawrzycka,[c] Grzegorz Bujacz,[d] Ulrich Haeberlen,[e] and Heike Schmitt[e]

Abstract: Bis[6-*O*,6-*O*′-(1,2:3,4-diisopropylidene-α-D-galactopyranosyl)thiophosphoryl] disulfide shows a strong tendency to form inclusion compounds. The crystal and molecular structure of eight different solvates was established by X-ray analysis. The results indicate three different types of disulfide arrangements in the crystal lattice. By means of ^{31}P CP/MAS NMR experiments the principal values δ_{11}, δ_{22}, and δ_{33} of the ^{31}P chemical shift tensor were obtained for each form. The orientation of its principal axes with respect to a molecular frame was investigated by means of ^{31}P CP and single-crystal NMR for the complex with propan-2-ol. The principal axis 1 of both chemically equivalent phosphorus atoms is nearly parallel to the P–S bond and the principal axis 3 is very close to the P=S bond. DFT GIAO calculations of the model compound $(EtO)_2(S)P^1SSP^2(S)(OEt)_2$ allowed assignment of the experimental chemical shift curves to the magnetically nonequivalent atoms P^1 and P^2. The maximum difference between calculated angles $(\measuredangle i\text{–P–X})_{calcd}$ and experimental angles $(\measuredangle i\text{–P–X})_{exptl}$ is 8.3° and the rms distance 3.8° (i = principal axes 1, 2, 3; X = S, -S-, -O1-, -O2-). The influence of C–H···S weak hydrogen bonding on phosphorus shielding was tested theoretically (^{31}P DFT GIAO) employing the dimethoxythiophosphoryl disulfide·CH_4 complex as a model compound. The sensitivity of ^{31}P δ_{ii} parameters to intermolecular forces is demonstrated.

Keywords: chemical shift tensor · density functional calculations · hydrogen bonds · inclusion compounds · solid-state structures

Introduction

Analysis of known crystal structures shows that only 15% of organic compounds are able to include solvent molecules in the solid state.[1] The formation of different structures depends on complex solute – solvent interactions. The thermodynamics in the process of crystallization of the host – guest compounds were recently discussed by Desiraju and co-workers.[2] The significance of noncovalent interactions (for example, strong and weak hydrogen bonds) and their influence on the crystal packing in these systems was also explored in detail.[3] Much attention was paid to the importance of weak C–H···O hydrogen bonding. Taylor and Kennard[4] showed that C–H···O contacts are electrostatic in nature and occur for C···O distances between 3.0 and 4.0 Å assuming that the C–H···O angle is in the range 90 – 180°. The geometry of C–H···O contacts in crystals of carbohydrates was reported by Steiner and Saenger.[5]

Investigating the bis[6-*O*,6-*O*′-(1,2:3,4-diisopropylidene-α-D-galactopyranosyl)thiophosphoryl] disulfide (**1**) we concluded that this molecule belongs to the rare class of compounds that have a very strong tendency to form inclusion complexes.[6, 7] A number of factors is responsible for the formation of different forms of **1**. Our attention was focused on possible P=S···H–C intermolecular contacts.[8, 9] The role of C–H···S hydrogen bonding and the influence of weak

[a] Doc. Dr. M. J. Potrzebowski, K. Ganicz, S. Olejniczak, W. Ciesielski
Department of Structural Studies
of the Centre of Molecular and Macromolecular Studies
Polish Academy of Sciences
Sienkiewicza 112, 90363 Łódź (Poland)
Fax: (+48) 42-6847126
E-mail: marekpot@bilbo.cbmm.lodz.pl

[b] Prof. Dr. G. Grossmann
Institut für Analytische Chemie
Technische Universität Dresden, 01062 Dresden (Germany)
E-mail: gisbert.grossmann@chemie.tu-dresden.de

[c] Prof. Dr. A. E. Kozioł, I. Wawrzycka
Marie Curie-Skłodowska University
20031 Lublin (Poland)

[d] Prof. Dr. G. Bujacz
Institute of Technical Biochemistry, Technical University
Stefanowskiego 4/10, 90924 Łódź (Poland)

[e] Prof. Dr. U. Haeberlen, H. Schmitt
Max-Planck-Institut für Medizinische Forschung
Jahnstrasse 29, 69120 Heidelberg (Germany)

  0947-6539/02/0812-2691 $ 20.00+.50/0

contacts on molecular packing of organic crystals was discussed by Borrmann et al.[10] A theoretical investigation of C–H···X hydrogen-bonded complexes (X = F, N, O, P, S) was recently reported by Radom and co-workers.[11]

We wished to find out the mechanism of the solute–solvent interactions in **1**, about the possible influence of P=S···H–C forces on NMR shielding parameters, and whether it is possible to learn the nature of such contacts by studying the tensorial character of the shielding of the ^{31}P nucleus. The project was carried out in several stages. In the first step, the crystal structures of different forms of **1** were established, and C–H···S and other intermolecular contacts were analyzed. In the second step, ^{31}P CP/MAS NMR experiments analyzed by the Herzfeld-Berger approach,[12] were used to find the values of the principal elements δ_{ii} of the ^{31}P chemical shift tensor for each complex. The next step was the measurement of the values of the principal elements of ^{31}P chemical shift tensors and the orientations of the principal axes with respect to a molecular frame by means of single-crystal NMR for the inclusion compound containing propan-2-ol in the crystal. Finally, the DFT GIAO method was used i) to assign the measured tensors to the two crystallographically equivalent, magnetically inequivalent phosphorus atoms in the unit cell, ii) to evaluate the accuracy of the calculated chemical shift tensors, and iii) to test the sensitivity of the δ_{ii} parameters to P=S···C–H contacts.

The GIAO B3PW91 hybrid method[13] was employed for calculating the ^{31}P shielding parameters. Unfortunately, calculation of the full structure of **1** is very time consuming and, because we were interested only in the NMR shielding parameters of the phosphorus atoms, we removed the sugar groups. These residues were replaced by ethoxy groups R^i **2**. The geometry of the $(R^iO)_2(S)PSSP(S)(OR^i)_2$ unit was kept exactly the same as that established by the single crystal X-ray studies of **1a**.

Bis(dimethoxythiophosphoryl) disulfide **3**·CH_4 complex was used as a model compound for the theoretical studies of P=S···H–C contacts. The compounds and models investigated in this work are summarized below.

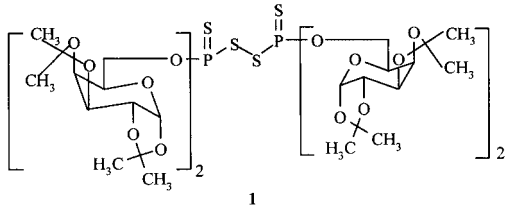

1

1a: **1** with propan-2-ol
1b: **1** with *n*-propanol
1c: **1** with diisopropyl ether
1d: **1** with toluene
1e: **1** with chloroform
1f: **1** with benzene and *n*-hexane
1g: **1** with benzene
1h: **1** with acetone
1i: **1** crystallized from methanol (without solvent in crystal lattice)
1j: **1** with methylcyclohexane

$(EtO)_2(S)PSSP(S)(OEt)_2$ (**2**)

$(MeO)_2(S)PSSP(S)(OMe)_2$ (**3**)

Results and Discussion

X-ray single crystal studies: In our previous work we found that bis[6-*O*,6-*O*′-(1,2:3,4-diisopropylidene-α-D-galactopyranosyl)thiophosphoryl] disulfide (**1**) crystallizes from polar as well as nonpolar solvents, for example from benzene, *n*-hexane, chloroform, acetone, and propan-2-ol, and forms different inclusion complexes.[6, 7] In this work we show that molecular complexes with propan-2-ol (**1a**),[7] propan-1-ol (**1b**), diisopropyl ether (**1c**) and toluene (**1d**) are isostructural (Table 1). These crystals are monoclinic, with the space group *C*2, and a host:guest ratio of 1:2. The disulfide bridge of the host molecule is located on a crystallographic twofold symmetry axis, thus the molecule in the solid state has the point symmetry C_2 (Figure 1).

The S=P, P–S bond lengths and the angles S=P–S and P–S–S–P in **1b**, **1c** and **1d** are almost identical, with respective values of about 1.9 (P=S), 2.08 Å (P–S), 106° (S=P–S) and |80|° (P–S–S–P) (Table 2). This geometry is characteristic for the S=PSSP=S fragment[6, 7] as well as *anti*–*anti* orientation of the S=P bonds (S=P–S–S is about −159°).[7] The values of torsion angles indicate that the galactopyranose ring in structures **1b**, **1c** and **1d** adopt a distorted twist-chair conformation.

Table 1. Crystallographic and experimental data for complexes **1b**–**d**.

	1b	**1c**	**1d**
empirical formula	$C_{24}H_{38}O_{12}PS_2/C_3H_8O$	$C_{24}H_{38}O_{12}PS_2/C_6H_{14}O$	$C_{24}H_{38}O_{12}PS_2/C_7H_8$
formula weight	673.73	715.81	705.77
crystal system	monoclinic	monoclinic	monoclinic
space group	*C*2	*C*2	*C*2
unit cell dimensions			
a [Å]	29.386(6)	30.762(6)	30.457(6)
b [Å]	10.430(2)	10.396(2)	10.372(2)
c [Å]	11.920(2)	12.017(2)	11.811(2)
β [°]	105.73(2)	93.48(3)	93.44(3)
V [Å^3]	3516.6(11)	3836.0(12)	3724.4(12)
Z	4	4	4
ρ_{calcd} [g cm^{-3}]	1.273	1.239	1.259
μ [mm^{-1}]	2.301	2.138	2.179
F(000)	1436	1532	1500
crystal size [mm]	0.49 × 0.16 × 0.1	0.62 × 0.23 × 0.1	0.83 × 0.23 × 0.49
θ range [°]	$3.12 \le \theta \le 67.24$	$2.88 \le \theta \le 80.37$	$2.91 \le \theta \le 80.38$
index ranges	$-33 \le h \le 11$	$0 \le h \le 39$	$-38 \le h \le 37$
	$-12 \le k \le 11$	$-13 \le k \le 0$	$-13 \le k \le 0$
	$-13 \le l \le 14$	$-15 \le l \le 15$	$-15 \le l \le 15$
reflections collected	5698	3668	7980
reflections independent	5081 ($R_{int} = 0.039$)	3614 ($R_{int} = 0.0366$)	4263 ($R_{int} = 0.071$)
data/restraints	5081/5	3614/23	4260/7
refined parameters	364	403	368
goodness of fit	1.025	1.021	1.054
R indices [$I > 2\sigma(I)$]	0.0571	0.0766	0.0497
wR_2	0.1427	0.1761	0.1222
R indices (all data)	0.0991	0.1608	0.1170
wR_2	0.1694	0.2241	0.1727
absolute structure parameter	0.03(3)	0.07(5)	0.09(3)
extinction coefficient	$1.2(2) \times 10^{-3}$	$0.8(2) \times 10^{-3}$	$1.5(2) \times 10^{-3}$
largest diff. peak, hole [e Å^{-3}]	0.52, −0.44	0.49, −0.35	0.26, −0.23

0947-6539/02/0812-2692 $ 20.00+.50/0 *Chem. Eur. J.* **2002**, *8*, No. 12

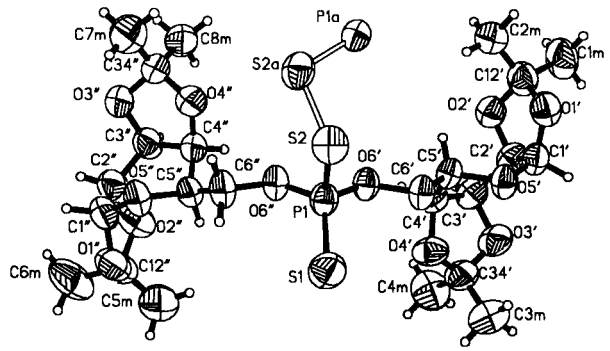

Figure 1. Molecular structure of the asymmetric unit of **1b** and the atomic numbering scheme.

Table 2. Selected bond lengths [Å], bond angles, and torsion angles [°].

	1b	**1c**	**1d**
P1–O6′	1.569(3)	1.568(6)	1.559(4)
P1–O6″	1.570(3)	1.555(6)	1.553(4)
P1–S1	1.898(2)	1.908(3)	1.900(2)
P1–S2	2.088(2)	2.075(4)	2.080(3)
S2–S2[a]	2.073(3)	2.068(6)	2.072(4)
S1-P1-S2-S2[a]	– 158.7(1)	– 158.6(2)	– 158.5(1)
P1-S2-S2[a]-P1[a]	– 79.3(1)	81.1(3)	– 80.4(2)

[a] Atoms are the symmetry equivalent atoms created by the twofold symmetry axis.

All crystals are built up of molecules of **1** packed along the twofold symmetry axes, and solvent molecules located around twofold screw axes. The guest molecules are locked in channels (parallel to the *b* axis) in which isopropylidene methyl groups of **1** are directed to the inside of channels causing steric hindrance. The dimension of a channel is about 8×13 Å, but the distance between methyl groups lying on the opposite walls of the channel is ≈ 6 Å. So, these groups are the main factor promoting the inclusion of guest molecules, even when no strong host···guest hydrogen bonds are formed. This conclusion is consistent with our NMR and DSC studies published elsewhere.[7]

In all structures, intermolecular C–H···S=P contacts are observed (Table 3): in **1b** and **1c** they are important components of both host···guest (shortest C···S distances are 3.88(4) and 3.52(2) Å for **1b** and **1c**, respectively), and host···host contacts, whereas in **1d** they link host molecules only (C···S 3.87(1) Å). Other attractive host···guest forces depend on the nature of the included solvent:

i) The propan-1-ol hydroxyl group in crystal **1b** is involved in a very weak O_{guest}–H···O_{host} hydrogen bond (geometry of this bond: O(1P)···O(1″) 3.345(3) Å, H(1O)···O(1″) 2.23 Å, ∢ O(1P)–H(1O)···O(1″) 110°).
ii) Weak hydrophobic C_{host}–H···π_{guest} interactions in crystal **1d** are observed between the toluene phenyl ring and the methine C–H group of the galactopyranose (with distances C···π 4.06 and H···π 3.11 Å).

Table 3. Geometry of C–H···S=P contacts (C···S1 < 4.1 Å).

	C···S1* [Å]	H···S1 [Å]	∢C-H···S1 [°]	(*) Symmetry code	Type of contact
1b	3.88(4)	3.03	152	½ – *x*, *y* – ½, – *z*	host···guest
	3.92(1)	3.13	141	*x*, *y*+1, *z*	host···host
	4.04(1)	3.12	162	*x*, *y*, *z* – 1	host···host
1c	3.52(4)	3.04	119		host···guest
	4.00(4)	3.75	94		host···guest
	4.07(2)	3.70	104		host···guest
	3.91(2)	3.15	136	*x*, *y* – 1, *z*	host···host
1d	3.87(1)	3.11	137	*x*, *y* – 1, *z*	host···host
	3.98(1)	3.06	160	*x*, *y*, *z* – 1	host···host

Inclusion crystals of **1** obtained from other solvents are built up of host molecules without the molecular twofold symmetry about the S–S bond.[6, 7] Their structures are: **1e** monoclinic, $P2_1$; **1f** orthorhombic, $P2_12_12_1$; **1g** and **1h** trigonal, $P3_2$.

However, the crystal lattice symmetry, the kind of guest molecule (polar or nonpolar) and its interactions with **1** have only a slight effect on host molecular geometry. A least-squares fit of the S=PSSP=S fragment of molecule **1**, adopting in the solid state eight inclusion compounds **1a**–**h**, showed that the molecular structures of the host molecules are very closed. The maximum deviation between respective atoms is 1.42 Å for **1g**, but between the four isostructural crystals **1a**–**d** the maximum deviation is only 0.82 Å.

This molecule is the basic building block of the solid-state structure. The common feature observed in each of crystals **1a**–**h** is the presence of molecular columns formed by **1** (Figure 2a): molecules aggregate in the "head-to-tail" mode, that is the disulfide bridge contact methyl groups of the opposite side of **1**, and they are repeated by a translation along the column. The translation period of 10.4–11.9 Å is simultaneously the length of the shortest of the unit-cell parameters. Different relative orientations of the columns in the three-dimensional crystal lattices depend on crystal symmetry. So far, three types of column packing have been observed (Figure 2b):

i) Columns are parallel in the space group *C*2.
ii) Columns are antiparallel, rotated by 180° in the space groups $P2_1$ and $P2_12_12_1$.
iii) Columns are rotated by 120° in the space group $P3_2$.

The included solvent molecules occupy free volumes between columns.

To check the importance of C–H···S=P intermolecular contacts, Version 5.21[14] of the CSD was used to search for geometrical data. The general search was performed for compounds containing C, H, O, S and P elements only, and for intermolecular C···S distances < 4.1 Å and C–H···S angles 90–180°. Among these structures, the subset of compounds with the S=P(O)$_2$–S fragment was found to have the shortest contacts (104 contacts in total); the minimal C···S contact is of 3.545(6) Å for 1,6-anhydro-2-*O*-tosyl-4-*S*-(5,5-dimethyl-2-thioxa-1,3,2-dioxaphosphorinan-2-yl)-β-D-glucopyranose propan-2-ol solvate at 85 K.[8]

^{31}P CP/MAS solid state NMR: The room-temperature ^{31}P CP/MAS spectra of bis[6-*O*,6-*O*′-(1,2:3,4-diisopropylidene-α-D-galactopyranosyl)thiophosphoryl] disulfide complexes **1b**, **c**, and **d** show one set of spinning sidebands from the large chemical-shielding anisotropy (CSA). The principal components δ_{ii} of the ^{31}P chemical shift tensors were calculated from the spinning sideband intensities employing the program WINMAS[15] that is based on the Herzfeld–Berger algorithm.[12] The isotropic chemical shifts δ_{iso} and the calculated values of δ_{ii} are given in Table 4. The accuracy of the

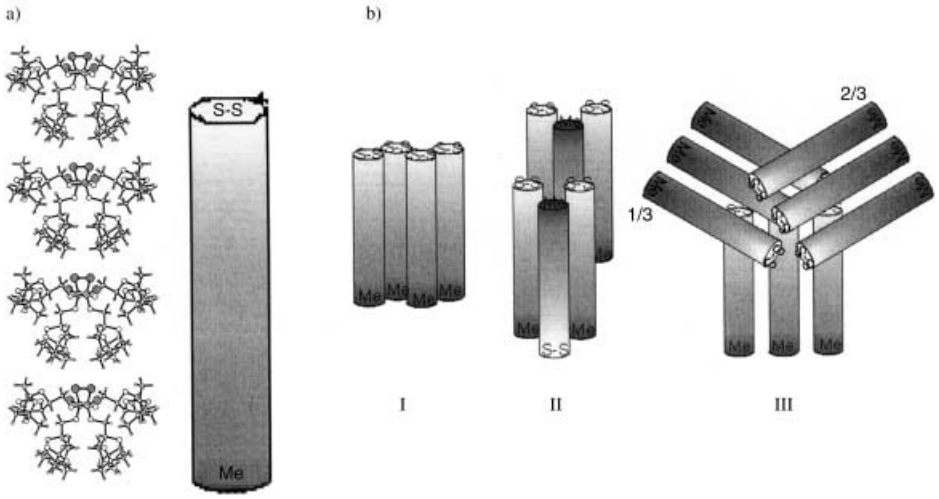

Figure 2. a) Packing of host molecules **1** within a column, and a symbolic description. b) Types of molecular column orientations of **1** observed in its inclusion complexes. I: parallel columns in the space group $C2$; II: antiparallel columns in the space groups $P2_1$ and $P2_12_12_1$; III: columns rotated by 120° in the space group $P3_2$.

Table 4. ^{31}P NMR chemical shift parameters for bis[6-*O*,6-*O*′-(1,2:3,4-diisopropylidene-α-D-galactopyranosyl) phosphorothioyl] disulfide (**1**).

Solvent	δ_{iso} [ppm]	δ_{11} [ppm]	δ_{22} [ppm]	δ_{33} [ppm]	References
2-propanol (**1a**)	83.4	194.3	99.3	−43.2	[7]
n-propanol (**1b**)	83.3	197.0	95.3	−42.4	this work
isopropyl ether (**1c**)	84.6	193.9	104.5	−44.6	this work
toluene (**1d**)	84.7	195.9	98.9	−40.6	this work
chloroform (**1e**)	88.0	200.2	103.2	−39.2	[8]
	85.9	200.4	96.2	−39.0	
benzene/*n*-hexane (**1f**)	86.8	196.6	105.0	−41.2	[8]
	86.2	197.1	102.0	−40.7	
benzene (**1g**)	89.1	203.5	102.8	−39.1	[8]
	86.5	199.7	101.8	−42.1	
acetone (**1h**)	86.2	197.6	97.1	−36.0	[7]
	84.2	191.2	91.5	−30.2	
without solvent (**1i**)	87.3	198.2	107.4	−43.8	this work
	84.0	190.8	102.6	−41.3	
methylcyclohexane (**1j**)	88.4	201.6	97.0	−33.4	this work
	87.5	205.4	104.4	−47.1	
	84.3	195.1	101.0	−43.3	
	82.4	196.4	95.2	−44.5	

calculations was verified by comparison with simulated spectra.

It is worth mentioning that ^{31}P CP/MAS NMR also offers the chance to test the ability of host molecule **1** to include solvents for phases of which we were not able to grow single crystals suitable for X-ray studies. Thus, Figure 3 displays the ^{31}P CP/MAS spectra of crystals of **1** obtained from methanol (**1i**) (without solvent in crystal lattice) and methylcyclohexane (**1j**) solutions.

It is known that the number of resonance lines in the isotropic part of such spectra provides information about the molecular content of the asymmetric unit. As concluded from ^{13}C CP/MAS measurements, sample **1i** does not contain solvent molecules in the crystal lattice. For this homomolecular system we can assume that one molecule is present in the asymmetric unit, and that two phosphorus centers P1 and P2 are distinguishable. The compound **1i** is only one example among others where the host **1** is not able to trap the guest molecule. Crystal **1j** presents a more complex picture with four ^{31}P NMR resonances in the isotropic part of the spectrum (Figure 3b). ^{13}C CP/MAS studies clearly show that methylcyclohexane is present inside the parent crystal lattice. Judging from the thermal instability of **1j**, which was also confirmed by a variable temperature (VT) ^{31}P CP/MAS investigation (Figure 3c), it can be assumed that solvent molecules are included only in part of the lattice of **1**. The less intensive outer lines in each sideband arise from crys-

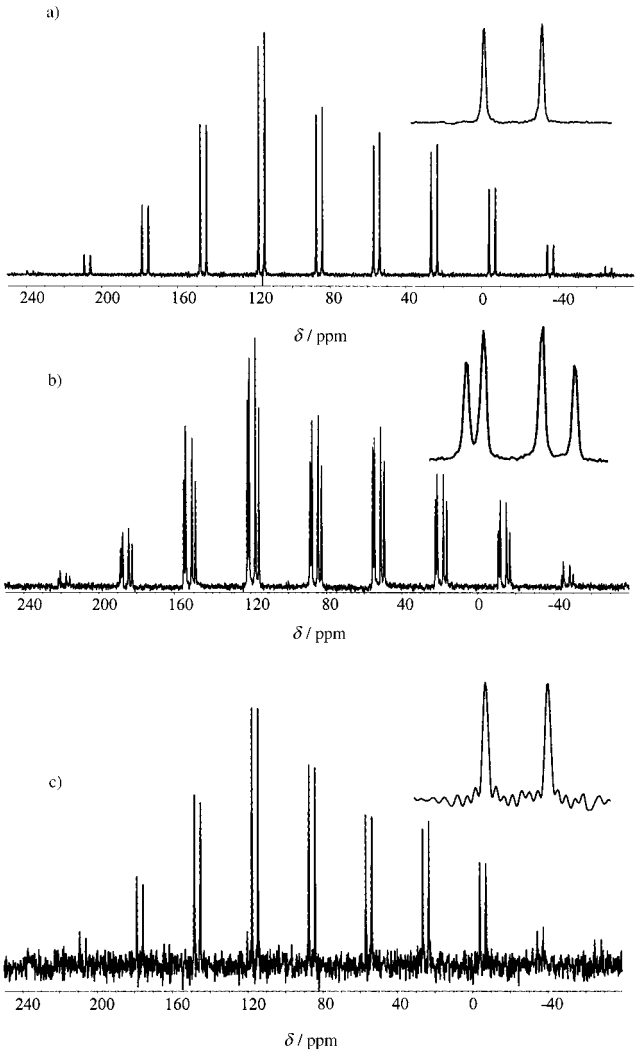

Figure 3. ^{1}H,^{31}P CP/MAS experimental spectra at 121.49 MHz of a) **1i** modification, b) **1j** modification, and c) modification of **1j** after heating. The spectra have 4 K data points with 10 Hz line broadening, a contact time of 1 ms, 100 scans and $\tilde{\nu}_{rot} = 3.7$ kHz.

0947-6539/02/0812-2694 $ 20.00+.50/0 *Chem. Eur. J.* **2002**, *8*, No. 12

tal ranges with included methylcyclohexane molecules while the more intensive inner lines correspond to solvent-free ranges. With an increase in temperature, a migration of the solvent molecules and a change of the crystal lattice is observed.

The ^{31}P δ_{ii} values for phases **1a–j** differ significantly (Table 4). A similar observation was recently reported for ^{13}C NMR by Smith et al. who investigated the polymorphism phenomenon of 5-methyl-2[(2-nitrophenyl)amino]-3-thiophenecarbonitrile by means of solid state ^{13}C 2D NMR techniques.[16] Grant and coworkers studied polymorphs of dimethyl-3,6-dichloro-2,5-dihydroxyterephtalane and found significant differences in the principal elements of the ^{13}C chemical shift tensors.[17] These authors concluded that conformational changes are responsible for the differences in the ^{13}C δ_{ii} parameters. Note, from our X-ray studies (see previous section) it follows that a change of the conformation of disulfide **1** cannot be responsible for the observed spread of the ^{31}P δ_{ii} values of its crystal structures.

It is known that conclusions regarding changes in the local environment of thiophosphoric systems can be drawn from an analysis of the principal components δ_{ii} of the ^{31}P chemical shift tensor.[18] The analysis of the data collected in Table 4 shows several intriguing features. All principal components δ_{ii} show differences up to $\Delta\delta_{ii} \approx 15$ ppm for the different forms. To explain such differences, we propose that they are due to weak hydrogen bonding to the thiophosphoryl group or to the bridging sulfur atoms. The origin of this effect is related to the change in electronic shielding of the phosphorus as the sulfur atoms becomes more polarized by the formation of the hydrogen bond. It is very hard to find an experimental method that could provide straightforward evidence for such subtle contacts as weak hydrogen bonding and, further, to find out how such contacts affect NMR parameters. On the other hand, very recently developed methods of quantum chemistry are a powerful tool for analysis of such problems. However, to discuss the question of P=S···H–C contacts in terms of the tensorial nature of the phosphorus shielding on the ab initio level, it is a prerequisite to know experimentally the orientation of the ^{31}P principal axes i with respect to a molecular frame of reference. The orientation of the principal axes remains hidden from MAS NMR investigations. This missing information can be obtained experimentally by NMR goniometer measurements of single crystals. Such NMR investigations were done only for a few phosphorus compounds,[19] because the measurements are time consuming, require a special probe head and a sufficiently large sample crystal with edges not smaller than 3 mm. In the following section we describe such measurements on the modification **1a**.

Single-crystal NMR of 1a: As crystals of **1a** are monoclinic with two crystallographically equivalent, magnetically inequivalent phosphorus atoms P1 and P2 in the unit cell (not counting translationally equivalent ones), its single crystal ^{31}P spectrum consists of a general orientation of the applied field B_0 of two chemically shifted resonances, which may, but need not, be split by the dipolar couplings of closest pairs of ^{31}P nuclei, see inset of Figure 4.

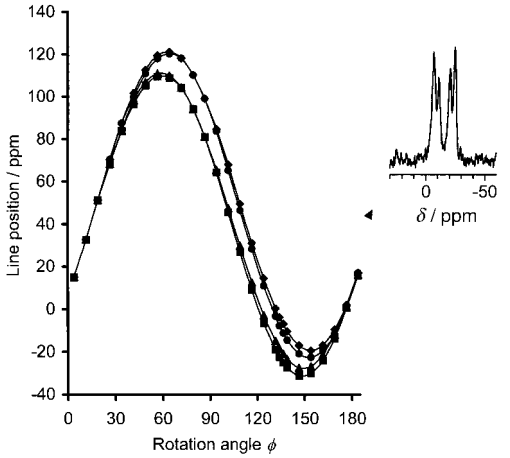

Figure 4. Angular dependence of the ^{31}P lines of a single crystal of **1a** from rotating the cube about the y_c axis. Inset: Spectrum for $\phi = 136.5°$ [note, it is a typical quasi-AB spectrum].

The dipolar splitting is given by $R(3\cos^2\theta - 1)$, where θ is the angle between the applied field B_0 and the line connecting the two P atoms. From the structure of **1a**, we deduce $R =$ 262 Hz. In general, such spectra will be determined by the difference of chemical shifts $(\tilde{\nu}_A - \tilde{\nu}_B)$ and by the direct and indirect spin-spin interactions. The $^3J_{PP}$ coupling, estimated from the solution ^{13}C NMR spectra of β and γ carbons are found to be below 2 Hz (this value is in accordance with that in other bis(dialkoxythiophosphoryl) disulfides[20]), and can be neglected in the analysis of solid-state single-crystal spectra with a line width over 250 Hz. If B_0 is either parallel to the monoclinic axis [010], or lies in the monoclinic plane (010) of the crystal, the resonances from P1 and P2 will collapse into a single one.

To access the symmetric parts of the chemical shift tensors of P1 and P2, we rotated an orientated single-crystal sample of **1a** fixed inside a hollow cube about the three cube edges labelled x_c, y_c, and z_c and took spectra for each 7.5° increment of the rotation angle. The rotation axis is, as usual, perpendicular to B_0. In Figure 4, the spectral positions of the observed lines are plotted for rotation of the sample about the y_c edge of the cube. The large variations of the line positions seen in that Figure are due to the anisotropic chemical shifts, the small splittings with their characteristic angular dependence due to the dipolar couplings. The centers of gravity of the dipolar split resonances, that is, the pure chemical shifts, are plotted in Figure 5 for rotation of the sample about the three cube edges x_c, y_c and z_c.

By a least-squares fitting procedure we want to analyse these so-called rotation patterns in terms of the chemical shift tensors σ of P1 and P2. In fact, only one shift tensor has to be determined because the second is symmetry related to the first. The important question is which of the two tensors is to be assigned to P1 and which to P2, and is beyond the pure data analysis so will be discussed further below.

For the data analysis we need to know the orientation of the sample crystal relative to the cube edges x_c, y_c and z_c. The plan was to fix the crystal inside the hollow cube such that the b axis, the $-c$ axis and the reciprocal axis a^* of the crystal, respectively, are parallel to the cube edges y_c, x_c and z_c. Had

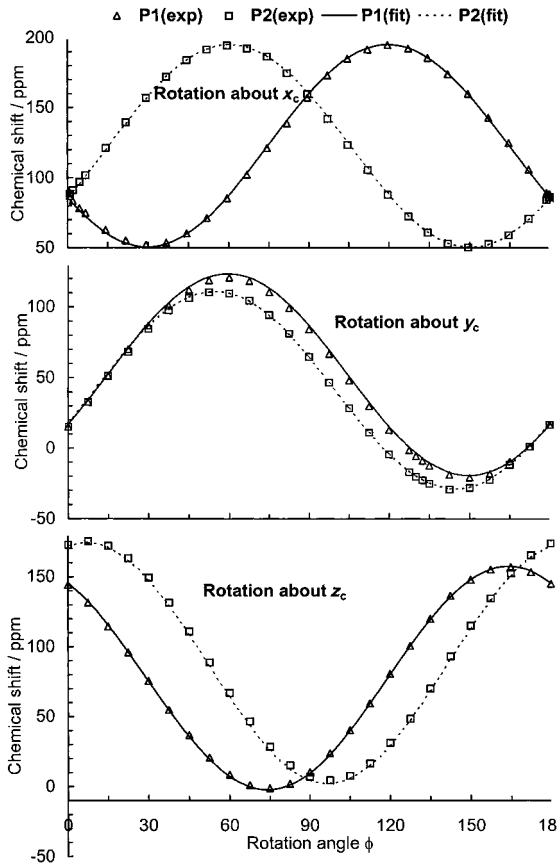

Figure 5. Angular dependence of the ^{31}P chemical shifts of a single crystal of **1a**. The curves reflect the fitted ^{31}P chemical shift tensors.

we succeeded perfectly, no chemical shift differences of P1 and P2 should be detectable in the y_c rotation pattern and, furthermore, the x_c and z_c patterns should be mirror symmetric about the crossings of the two traces in these patterns. As Figure 5 shows, these criteria are satisfied approximately, but not perfectly. As the x_c pattern displays nearly perfect mirror symmetry we concluded that the x_c edge of the cube lies very close to the monoclinic plane (010) of the crystal. To start the data analysis we assume that it is, as planned, parallel to $-c$. The data in Figure 5 are highly redundant for determining the six cartesian components σ_{ij} ($=\sigma_{ji}$) of the symmetric part of a chemical shift tensor in a suitable chosen crystal-fixed axes system for which we use the so-called standard orthogonal system (SOS) with $x_{SOS} \parallel a$, $y_{SOS} \parallel b$ and $z_{SOS} \parallel c^*$. Therefore, we can use these data for improving our knowledge of the orientation of the sample crystal inside the cube. The possible improvement concerns primarily the orientation of the y_c and z_c cube edges inside the plane perpendicular to $-c$. This orientation is described by the (signed) angle $\alpha = \sphericalangle(b, y_c)$. We point out that the data do not allow us, unfortunately, to detect and correct a deviation of the cube edge x_c from $-c$ so long as x_c remains within the monoclinic plane (010).

Fitting is done with the second-rank tensor least-squares fitting program SUPERFIT.[21] Apart from shift data as in Figure 5, SUPERFIT needs as input (i) the orientation of the rotation axis R of each pattern specified by, for example, its polar angles ϑ_R and φ_R in the SOS and, ii) a reference angle ϕ_R for which rotation angle ϕ the applied field B_0 is parallel to a specified reference direction in the plane perpendicular to the rotation axis. By inspection of the x_c and z_c patterns in Figure 5 we can safely conclude that the crossing of the two traces at the common value of about $\delta = 160$ must correspond to B_0, approximately parallel to b. Therefore, the other crossings of the traces (at about $\delta = 88$ in the x_c pattern and at about $\delta = 8$ in the z_c pattern) and also the (single) crossing of the traces in the y_c pattern must correspond to crossings of the path $B_0(R_i,\phi)$, $R_i = x_c, y_c, z_c$, with the monoclinic plane (010) of the crystal. The direction of B_0 at a crossing point is fixed once the rotation axis of the crystal is known and we take that direction as the reference direction for SUPERFIT. The corresponding reference angles $\phi_r^{(R_i)}$ can be read from the rotation patterns with considerable accuracy.

SUPERFIT calculates for a test tensor σ^{test} the shifts for all crystal orientations implied by data as in Figure 5 and minimizes with respect to the components σ_{ij}^{test} the standard deviation sigma of the (weighted) squares of the differences between calculated and actually measured shifts. In the present data analysis we also considered α as a free parameter to minimize sigma. The best-fit value for α turned out to be $\alpha_{opt} = -5.0^\circ$. After the fitting procedure had converged, we still noticed deviations between calculated and observed shifts, which were systematic with respect to the rotation angle ϕ in the three rotation patterns. We tried to eliminate them by allowing x_c to move out of the monoclinic plane (010) by an angle β. A slightly smaller minimum of sigma was reached for $\beta = 1.0^\circ$ but systematic differences remained. We think they are due to the assumed orthogonality of the three rotation axes implied by our data analysis, which in reality need not be exactly true. The result of the fit is given in Table 5. Its quality may be appreciated by comparing the data points in Figure 5 with the full curves, which represent the fitted tensors. Included in Table 5 are δ_{iso} and the principal values σ_{ii} as obtained from a side band analysis of CP/MAS experiments, as well as results from DFT GIAO calculations to which we turn now.

Table 5. Experimental and calculated ^{31}P nuclear magnetic shielding tensors of **1a** characterized by principal values σ_{ii} [ppm][a] and orientations of the principal axes i in the SOS.[b]

Method	δ_{iso}	σ_{11}	σ_{22}	σ_{33}	rms distance [ppm][c]	
CP/MAS [d]	83.4	133.7	228.7	371.2	1.3	
single crystal	84.1	132.8	229.7	369.3	1.5[e]	
DFT GIAO[f]	101.6	111.4	199.7	368.0	21.3	
	axis 1		axis 2		axis 3	
	θ_1	φ_1	θ_2	φ_2	θ_3	φ_3
single crystal	81.77	61.28	40.98	321.70	129.79	338.20
DFT GIAO	77.92	63.02	34.47	314.85	121.72	340.63

[a] $\sigma_{ii} = 328$ ppm $- \delta_{ii}$, see ref. [22]. The δ_{ii} are referenced to H_3PO_4 (85%). [b] The polar angles θ_i and the azimuth angles φ_i define the orientation of the principal axis i for atom P1 in the standard orthogonal system: $x_{SOS} \| a$; $y_{SOS} \| b$; $z_{SOS} \| c^*$. For atom P2 these angles amount to $\theta_i(2) = 180^\circ - \theta_i(1)$ and $\varphi_i(2) = 180^\circ - \varphi_i(1)$. [c] rms distance $= \{[\Sigma(A_{j,x} - A_{j,s})^2]/n\}^{1/2}$, with $A - n$ values, $i = 1 \ldots n$, x: MAS NMR values or DFT GIAO values, s: single crystal NMR values. [d] See ref. [7]. [e] The standard deviation s of the fitting procedure for single-crystal measurements. [f] For model compound **2**.

0947-6539/02/0812-2696 $ 20.00+.50/0 *Chem. Eur. J.* **2002**, *8*, No. 12

As mentioned above, there is no purely experimental way to assign the chemical shift tensor specified in Table 5 to either P1 or P2. To learn which assignment is correct we performed chemical shift tensor calculations using the DFT GIAO approach included in the Gaussian 98 program package.[13] Rather than perform the calculations for the complicated molecule **1a**, we did them for the simpler model compound **2**. In ref. [19h] we showed that such model calculations lead to only slightly poorer results than calculations for the larger molecule of actual interest. According to the calculations, the principal axis 3 (most shielded) is expected to be very close to the P=S double bond while principal axis 1 (least shielded) should be close to the P–S single bond. Indeed, one and only one of the two possible assignments reflects these shielding characteristics such that we can safely conclude that the tensor specified in Table 5 is to be assigned to P1. Following this assignment we show the relation of the principal axes 1, 2 and 3 of the ^{31}P chemical shift tensor to the molecular framework of **1a**. In Table 6 we list the angles subtended by the principal ^{31}P shielding axes 1, 2 and 3 and all bonds of the phosphorus atom P1 in **1a** as they are found in the experiment and, in the model compound **2**, by the DFT GIAO calculation. The root-mean-square-distance between the measured and calculated angles is 3.8°, which confirms the adequacy of the calculation for the purpose of the tensor assignment.

Table 6. Angles between principal axes *i* and P–X bonds from a single crystal of **1a** and calculated values for the model compound **2**.[a] The shaded entries demonstrate that the principal axis 3 is nearly parallel to the P=S bond while the principal axis 1 is nearly parallel to the P–S bond.

Method	*i*	∢ *i*–P=S	∢ *i*–P–S	∢ *i*–P–O1	∢ *i*–P–O2
single crystal	1	93.6	14.2	110.1	120.5
	2	89.5	96.7	38.7	134.9
	3	3.7	102.5	121.5	119.6
DFT GIAO	1	89.9	17.0	113.7	121.1
	2	97.0	92.8	34.2	131.0
	3	7.0	106.8	113.2	123.4

[a] rms distance $= \{\Sigma\,[(\sphericalangle i\text{–P–X})_{calcd} - (\sphericalangle i\text{–P–X})_{exp}]^2 \cdot 1/12\}^{1/2} = 3.8°$.

^{31}P DFT GIAO calculation of P–S···H–C contacts: We now turn to the influence of P=S···H–C contacts on ^{31}P shielding parameters. In order to analyse this problem within a reasonable time and with sufficient accuracy, we employed an even simpler model, bis(dimethoxythiophosphoryl) disulfide **3**, for which the X-ray structure and preliminary ^{31}P CP/MAS studies were published previously.[23, 24] This compound crystallizes in the space group *C*2/*c* with one molecule in the asymmetric unit. The experimental isotropic ^{31}P resonances of P1 and P2 are separated by 3.0 ppm. As coordinates for calculation of the model compound **3** we have used the crystal structure data of the real molecule. We may conclude that the orientation of the ^{31}P principal axes in the molecular frame is the same as in the case of **2**.

In the next step, we built the molecular complex shown in Figure 6a, where the methane molecule is in close proximity to one of the thiono-sulfurs of **3** and the P1=S···H–C unit is aligned in the plane of S=P1–S bonds. The distance *d* between the sulfur and the carbon in the P1=S···H–C fragment was

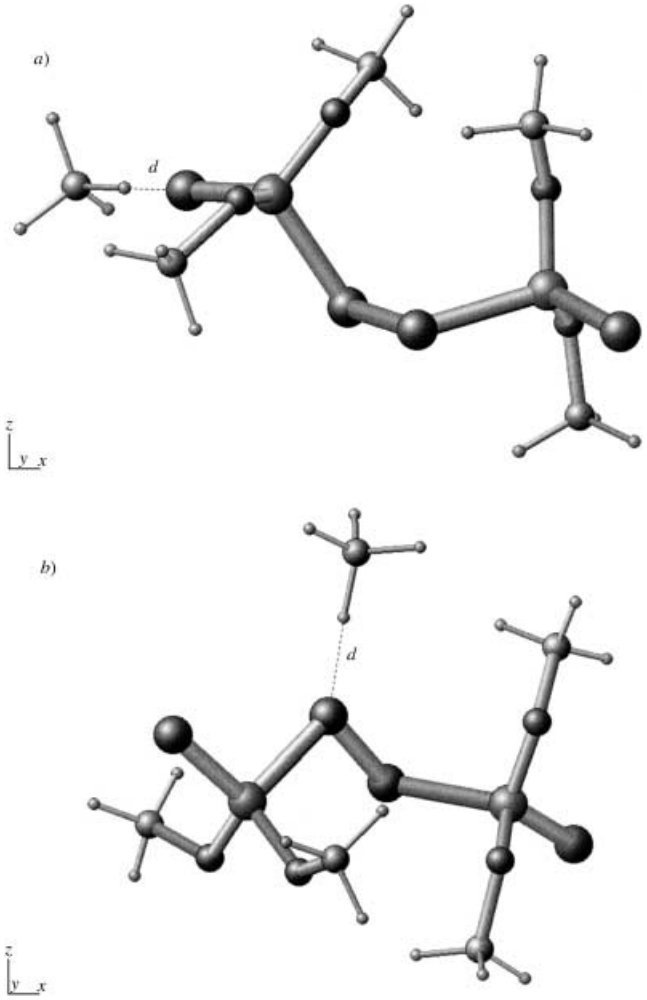

Figure 6. The molecular complex of bis(dimethoxythiophosphoryl) disulfide **3** with methane.

varied in the range from 2.4–4.1 Å. Several DFT GIAO calculations were carried out with constant increments of *d* equal to 0.1 Å. When *d* is equal to 4.0 Å, the shielding parameters for both centers P1 and P2 are the same as in the isolated molecule **3**. The calculated isotropic ^{31}P resonances of P1 and P2 are separated by 2.2 ppm. The results of the calculations for P1 are presented in Figure 7a. With decreasing *d* a change of the δ_{ii} for P1 takes place while these values for P2 remain practically constant. It is interesting to note that the changes of σ_{11} and σ_{22} on the one hand, and σ_{33} on the other, go in opposite directions: with increasing σ_{11} and σ_{22} a decrease of σ_{33} is observed. When *d* is in the range of 3.2–3.8 Å (the region of interest) the changes of σ_{11} and σ_{33} amount to a few parts per million.

Finally, we were attracted by the prospect of establishing the influence of P1–S···H–C forces on ^{31}P NMR shielding parameters considering the thiolo sulfur. The model used for such a calculation is presented in Figure 6b. Figure 7b shows the relationship between *d* distance and σ_{ii} values for P1. Analysis of the data obtained shows that the influence of this type of interaction on ^{31}P NMR shielding is much smaller compared to analogous thiono sulfur···CH_4 contacts. This fact is apparent from comparison of changes of span Ω

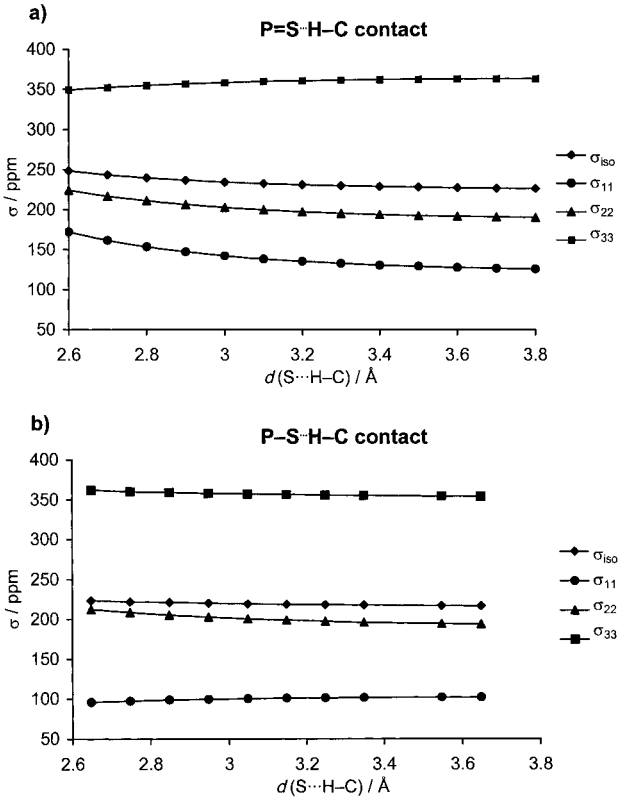

Figure 7. The relationship between the distance d between the sulfur and the carbon in the P=S···H–C and the P–S···H–C units and the values of the principal elements of the ^{31}P nuclear magnetic shielding tensors calculated by the DFT GIAO method.

parameters[25] defined as $\sigma_{33}-\sigma_{11}$ versus d as shown in Figure 8.

As known, the inner shell electrons contribute to a strong and nearly isotropic shielding of a nucleus, while the valence electrons give anisotropic deshielding contributions. If one considers that the deshielding contributions to a given σ_{ii} depend on the electronic structure in a plane perpendicular to the principal axis i, bonds almost perpendicular to a certain principal axis i should mainly affect the magnitude of σ_{ii}. This effect is well demonstrated by the LMO contributions of IGLO calulations.[26] The considered P=S···H–C interactions lie in the direction of the principal axis 3 and the distortion of the electronic structure of molecule **3** results in a decrease of deshielding in σ_{11} and σ_{22} and a increase in σ_{33} while the P–S···H–C interactions lie in the direction of the principal axis 1 and the distortion of the electronic structure results in a decrease of deshielding in σ_{22} and σ_{33} and an increase in σ_{11}. Therefore, the curves in Figure 8 show an opposite slope.

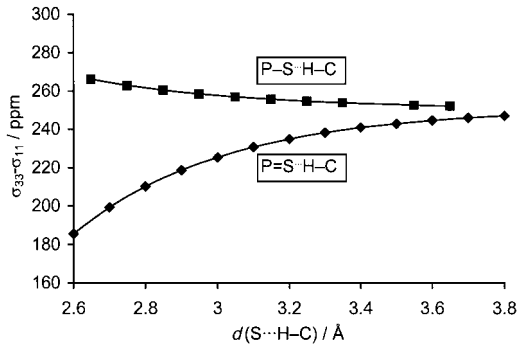

Figure 8. Comparison of changes of the span parameter ($\Omega=\sigma_{33}-\sigma_{11}$) of the ^{31}P nuclear magnetic shielding tensors calculated by the DFT GIAO method versus the distance d between the sulfur and the carbon in the P=S···H–C and the P–S···H–C units.

Conclusion

In this work the nature of solute–solvent interactions in solid dithiophosphoroorganic carbohydrate derivative **1** is discussed. From X-ray studies it is apparent that the most important factor responsible for holding guest molecules in the crystal lattice is the van der Waals force together with steric complementarity between host cavity and guest. The importance of the packing coefficient of host cavities was discussed recently by Nakano et al.[27] For **1**, the barrier caused by methyl groups of the isopropylidene blocking group is crucial. The cases of methanol and ethanol, which are too small to be trapped in the channels of **1**, are very convincing.

Intermolecular interactions other than van der Waals forces can be considered as a secondary factor, which operates when the first condition is fulfilled. This synergistic mechanism seems to be especially important for **1** and is responsible for its high affinity for host–guest complex formation. The combination of experimental and theoretical approaches gives a full picture of the nature of such contacts. The single-crystal NMR studies provide the necessary information about the orientation of the principal axes of the chemical shift tensors with respect to the molecular frame of **1**. From our ^{31}P CP/MAS measurements and DFT calculations it became clear that the δ_{ii} components are sensitive to P=S···C–H hydrogen bonding. The analysis of the whole set of ^{31}P δ_{ii} parameters gives much more information about the nature of such contacts than the inspection of only the isotropic values. In particular, the span parameter defined as the difference between σ_{33} and σ_{11} gives straightforward information about the strength of C–H···S hydrogen bonding.

Experimental Section

Preparations: Compound **1**[7] (100 mg) was dissolved by warming in the liquid guest (usually 5 mL), and the resulting solution allowed to stand at room temperature. The crystals obtained were collected and dried on filter paper.

X-ray Studies: Crystal data and experimental details are displayed in Table 1. Diffraction data were measured at room temperature on a KM4 diffractometer using $Cu_{K\alpha}$ radiation ($\lambda=1.54178$ Å). Crystal structures were solved by direct methods (SHELXS-97)[28] and refined by full-matrix least-squares minimization on F^2 using the program SHELXL-93[29a] for **1b** and **1d**, and SHELXL-97[29b] for **1c**. The starting coordinates used in the refinement were those for the enantiomer of **1** having the known configuration of D-galactopyranose. Non-H atoms of the host molecules were refined with anisotropic thermal parameters. Solvent molecules are disordered or poorly localized. Thus, for toluene and diisopropyl ether, non-H atoms coordinates and isotropic displacement parameters were refined, and for propan-1-ol non-H atoms positions only were refined, isotropic thermal factors were kept fixed at $U_{iso}=0.5$ Å^2. Moreover, bond length restraints were applied to all guest molecules. Methyl groups of diisopropyl ether were found to be rotationally disordered with an

  0947-6539/02/0812-2698 $ 20.00+.50/0 *Chem. Eur. J.* **2002**, *8*, No. 12

occupation ratio 0.6:0.4. Hydrogen atoms of host, toluene, and diisopropyl ether were positioned geometrically and their isotropic displacement parameters were set to $U_{iso} = 1.2\ U_{eq}$ of the C-atom to which they are bonded, while isotropic displacement parameters of all H-atoms of propan-1-ol were set to $U_{iso} = 0.55$ Å^2.

CCDC-172522, 172523, and 172524 contain the supplementary crystallographic data for this paper. These data can be obtained free of charge via www.ccdc.cam.ac.uk/conts/retrieving.html (or from the Cambridge Crystallographic Data Centre, 12 Union Road, Cambridge CB2 1EZ, UK; fax: (+44) 1223-336033; or e-mail: deposit@chemcrys.cam.ac.uk).

CP/MAS NMR Spectroscopy: Cross-polarization magic angle spinning solid state ^{31}P NMR spectra were recorded at 121.46 MHz on a Bruker 300 DSX instrument with proton decoupling. Powder samples of **1** were placed in a cylindrical rotor and spun at 2.0–4.5 kHz. The field strength for ^{1}H decoupling was 1.05 mT, a contact time of 5 ms, a repetition delay of 6 s, and a spectral width of 50 kHz were used, and 8 K data points represented the FID. Spectra were accumulated 500 times, giving a reasonable signal-to-noise ratio. ^{31}P chemical shifts were calibrated indirectly through bis(dineopentoxyphosphorothioyl) disulfide set at $\delta = 84.0$.

The principal elements of the ^{31}P chemical shift tensor were calculated with the program WINMAS.[15] Details describing the method and the accuracy of calculations are exhaustively discussed elsewhere.[30]

Single-crystal ^{31}P NMR spectroscopy: A special probe made by G. Scheler, Jena (Germany), equipped with a goniometer and working at 121.5 MHz on BRUKER widebore 7.1 T magnets was used. ^{1}H high-power decoupling coils were added by BRUKER. The rod for crystal rotation contains a cubic hole to pick up an open $3 \times 3 \times 3$ mm^3 cube as crystal holder to which the crystal was fixed with its largest face, the 100 plane. The approximate orientation $x_c || -c, y_c || b$ and $z_c || a^*$ of the monoclinic crystal relative to the cube axes x_c, y_c and z_c was controlled by X-rays. Three series of measurements were carried out by rotating the crystal about the three cubic axes from 0–180° perpendicular to B_0 in steps of 7.5°. Duration of $\pi/2$ pulse: 11 μs; dwell time: 9.1 μs; number of samples/fid: 2048; recycle delay: 6 s; number of accumulations per spectrum: 500–1000.

Calculations: The primary calculations were performed on the model compound $(EtO)_2(S)P^1SSP^2(S)(OEt)_2$. The coordinates of the corresponding atoms were adopted from the crystal structure **1a**.[7] Geometry optimization was allowed for the hydrogen atoms only. The influence of P=S···H–C contacts on the principal values δ_{ii} of the ^{31}P shielding tensor was simulated employing $(MeO)_2(S)P^1SSP^2(S)(OMe)_2 \cdot CH_4$ complexes as model compounds. In the DFT part of GAUSSIAN 98[13] the B3LYP functionals and the 6-31+G** basis sets were used. Calculation of the nuclear magnetic shielding tensors was by the GIAO method.

Acknowledgements

This work was supported by the Polish Committee for Scientific Research, KBN, grant no. 3 T09A 02619. G.G. acknowledges the European Community's Centers of Excellence program for financial support for his one month stay in Łódź.

[1] A. Nangia, G. R. Desiraju, *Chem. Commun.* **1999**, 605.
[2] V. S. S. Kumar, S. S. Kuduva, G. R. Desiraju, *J. Chem. Soc. Perkin Trans. 2* **1999**, 1069.
[3] a) J. Stezowski, W. Parker, S. Hilgenkamp, M. Gdaniec, *J. Am. Chem. Soc.* **2001**, *123*, 3919; b) D. V. Soldatov, J. A. Ripmeester, *Chem. Eur. J.* **2001**, *7*, 2979.
[4] R. Taylor, O. Kennard, *J. Am. Chem. Soc.* **1982**, *104*, 5063.
[5] T. Steiner, W. Saenger, *J. Am. Chem. Soc.* **1992**, *114*, 10146.
[6] M. J. Potrzebowski, J. Błaszczyk, M. W. Wieczorek, *J. Org. Chem.* **1995**, *60*, 2549.
[7] M. J. Potrzebowski, K. Ganicz, W. Ciesielski, A. Skowronska, M. W. Wieczorek, J. Blaszczyk, W. Majzner, *J. Chem. Soc. Perkin Trans. 2* **1999**, 2163.
[8] M. J. Potrzebowski, M. Michalska, A. E. Kozioł, S. Kazmierski, T. Lis, J. Pluskowski, W. Ciesielski, *J. Org. Chem.* **1998**, *63*, 4209.
[9] M. J. Potrzebowski, X.-B. Yang, K. Misiura, S. Kazmierski, S. Olejniczak, W. R. Majzner, M. W. Wieczorek, W. J. Stec, *Eur. J. Org. Chem.* **2001**, 1491.
[10] H. Borrmann, I. Persson, M. Sandström, C. M. V. Stålhandske, *J. Chem. Soc. Perkin Trans. 2* **2000**, 393.
[11] M. Hartmann, S. D. Wetmore, L. Radom, *J. Phys. Chem. A* **2001**, *105*, 4470.
[12] J. Herzfeld, A. E. Berger, *J. Chem. Phys.* **1980**, *73*, 6021.
[13] Gaussian 98, Revision A.6, M. J. Frisch, G. W. Trucks, H. B. Schlegel, G. E. Scuseria, M. A. Robb, J. R. Cheeseman, V. G. Zakrzewski, J. A. Montgomery, Jr., R. E. Stratmann, J. C. Burant, S. Dapprich, J. M. Millam, A. D. Daniels, K. N. Kudin, M. C. Strain, O. Farkas, J. Tomasi, V. Barone, M. Cossi, R. Cammi, B. Mennucci, C. Pomelli, C. Adamo, S. Clifford, J. Ochterski, G. A. Petersson, P. Y. Ayala, Q. Cui, K. Morokuma, D. K. Malick, A. D. Rabuck, K. Raghavachari, J. B. Foresman, J. Cioslowski, J. V. Ortiz, B. B. Stefanov, G. Liu, A. Liashenko, P. Piskorz, I. Komaromi, R. Gomperts, R. L. Martin, D. J. Fox, T. Keith, M. A. Al-Laham, C. Y. Peng, A. Nanayakkara, C. Gonzalez, M. Challacombe, P. M. W. Gill, B. Johnson, W. Chen, M. W. Wong, J. L. Andres, C. Gonzalez, M. Head-Gordon, E. S. Replogle, J. A. Pople, Gaussian, Inc., Pittsburgh PA, **1998**.
[14] F. H. Allen, O. Kennard, *Chem. Design Automation News* **1993**, *8*, 31 (Version 5.21).
[15] WIN-MAS program, version 940108, Bruker-Franzen Analytik, Bremen, **1994**.
[16] J. Smith, E. MacNamara, D. Raftery, T. Borchardt, S. Byrn, *J. Am. Chem. Soc.* **1998**, *120*, 11710.
[17] M. Strohmeier, A. M. Orendt, D. W. Alderman, D. M. Grant, *J. Am. Chem. Soc.* **2001**, *123*, 1713.
[18] T. Kuivalainen, J. El-Bahraoui, R. Uggla, R. Kostianen, M. R. Sundberg, *J. Am. Chem. Soc.* **2000**, *122*, 8073, and references therein.
[19] a) S. J. Kohler, M. P. Klein, *J. Am. Chem. Soc.* **1977**, *99*, 8290; b) P. Tutunjian, J. Tropp, J. Waugh, *J. Am. Chem. Soc.* **1983**, *105*, 4848; c) M.-R. Van Calsteren, G. J. Birnbaum, I. C. P. Smith, *J. Chem. Phys.* **1987**, *86*, 5405; d) C. A. McDowell, A. Naito, D. L. Sastry, K. Takegoshi, *J. Magn. Reson.* **1988**, *78*, 498; e) H. Hauser, C. Radloff, R. R. Ernst, S. Sundell, I. Pascher, *J. Am. Chem. Soc.* **1988**, *110*, 1054; f) J. Rohonczy, F. Ermark, U. Haeberlen, G. Klose, M. Schulz, *Chem. Phys. Lett.* **1991**, *180*, 23; g) K. Eichele, R. E. Wasylishen, J. F. Corrigan, N. J. Taylor, A. J. Carty, *J. Am. Chem. Soc.* **1995**, *117*, 6961; h) G. Grossmann, D. Scheller, O. L. Malkina, V. G. Malkin, G. Zahn, H. Schmitt, U. Haeberlen, *Solid State NMR* **2000**, *17*, 22; i) M. Bechmann, S. Dusold, H. Förster, U. Haeberlen, T. Lis, A. Sebald, M. Stumber, *Mol. Phys.* **2000**, *98*, 605.
[20] H. Komber, G. Grossmann, A. Kretschmer, *Phosphorus Sulfur* **1988**, *35*, 335.
[21] H. Schmitt, H. Zimmermann, O. Körner, M. Stumber, C. Meinel, U. Haeberlen, *J. Magn. Reson.* **2001**, *151*, 65.
[22] C. J. Jameson, A. C. de Dios, A. K. Jameson, *Chem. Phys. Lett.* **1990**, *167*, 574.
[23] M. J. Potrzebowski, J. H. Reibenspies, Z. Zhong, *Heteroatom Chem.* **1991**, *2*, 455.
[24] P.-J. Chu, M. J. Potrzebowski, *Magn. Reson. Chem.* **1990**, *28*, 477.
[25] J. Mason, *Solid State NMR* **1993**, *2*, 285.
[26] G. Grossmann, H. Beckmann, O. Rademacher, K. Krüger, G. Ohms, *J. Chem. Soc. Dalton Trans.* **1995**, 2797.
[27] K. Nakano, K. Sada, Y. Kurozumi, M. Miyata, *Chem. Eur. J.* **2001**, *7*, 209.
[28] G. M. Sheldrick, SHELXS-97: Program for crystal structure solution, University of Göttingen (Germany), **1997**.
[29] a) G. M. Sheldrick, SHELXL-93: Program for the refinement of crystal structures from diffraction data, University of Göttingen (Germany), **1993**; b) G. M. Sheldrick, SHELXL-97: Program for the refinement of crystal structures from diffraction data, University of Göttingen (Germany), **1997**.
[30] G. Jeschke, G. Grossmann, *J. Magn. Reson.* **1993**, *A 103*, 323–328.

Received: November 9, 2001 [F3674]

  0947-6539/02/0812-2699 $ 20.00+.50/0